

Time Relationships between Direct Particle Emission and Fragmentation: A Probe for Nuclear Expansion Prior to Fragment Freeze-Out

C. J. Gelderloos,^{1,*} John M. Alexander,¹ N. N. Ajitanand,¹ E. Bauge,^{1,2} A. Elmaani,^{1,†} T. Ethvignot,^{1,2,‡} L. Kowalski,¹ Roy A. Lacey,¹ M.E. Brandan,^{2,§} A. Giorni,² D. Heuer,² S. Kox,² A. Lleres,² A. Menchaca-Rocha,^{2,‡} F. Merchez,² D. Rebreyend,² J. B. Viano,² B. Chambon,³ B. Cheynis,³ D. Drain,³ and C. Pastor³

¹*Departments of Physics and Chemistry, State University of New York at Stony Brook, Stony Brook, New York 11794*

²*Institut des Sciences Nucléaires de Grenoble, Institut National de Physique Nucléaire et de Physique des Particules-Centre National de la Recherche Scientifique/Université Joseph Fourier, 53 Avenue des Martyrs, 38026 Grenoble Cedex, France*

³*Institut de Physique Nucléaire de Lyon, Institut National de Physique des Particules-Centre National de la Recherche Scientifique/Université Claude Bernard, 43, Boulevard du 11 Novembre 1918, 69622 Villeurbanne Cedex, France*

(Received 17 August 1994; revised manuscript received 8 March 1995)

A previously unexploited experimental observable is used to explore emission times for intermediate mass fragments relative to directly emitted ^2H and ^3H particles. Small-angle correlations are reported in central collisions for 34A MeV $^{40}\text{Ar} + ^{\text{nat}}\text{Ag}$. High-velocity ^3H and ^2H particles follow a direct emission scenario with mean lifetime $\tau \sim 30\text{--}60$ fm/c. Fragmentation to Li is characterized by $\tau \sim 120$ fm/c. Current model calculations suggest a delay time of $\sim 100\text{--}200$ fm/c for expansion of the central collision zone prior to the onset of "freeze-out" into fragments. But the observed velocity difference spectra limit the delay time to ≤ 50 fm/c for expansion between direct emission and fragmentation.

PACS numbers: 25.70.Pq

At excitation energies of 5–6 MeV/nucleon and above, current reaction models often include the theme of collisional compression and subsequent expansion, prior to low-density "freeze-out" and multifragment emission (see, e.g., [1–5]). Microscopic model calculations (by molecular dynamics as well as those based on a transport equation) suggest that fragment production from an expanded nuclear system would require a time delay of $\sim 100\text{--}200$ fm/c after the initial impact between target and projectile, e.g., [1–4]. To date, no convincing experimental signature has been found for such behavior, although it is widely assumed to be valid. However, if the time scale and/or the initiation time for fragment emission differ from that for direct particle emission, then a crucial experimental observable could be the average ejectile emission order for these two reaction classes. In this paper we present the first experimental results sensitive to both the emission order and time delays between fragments and direct particles produced in the most violent collisions of 1360 MeV ^{40}Ar with Ag [6,7]. Fragmentation, in this reaction, cannot be accounted for by a scenario of freeze-out from an expanded and thermalized nucleus. Instead, the fragmentation seems to be better described as a prethermalization process.

The particular reaction we employ here, 34A MeV $^{40}\text{Ar} + ^{\text{nat}}\text{Ag}$, is one that has been studied a great deal [8–12]. Estimates of the initial excitation energy in central collisions are $\sim 5\text{--}6$ MeV/nucleon with a corresponding temperature of ~ 7 MeV. Light-charged particle ($Z = 1, 2$) emission from the more central collisions is typified by invariant cross sections and angular and energy distributions, which exhibit nearly isotropic emission (for $\theta_{\text{lab}} \gtrsim 60^\circ$) from a source moving with

an average velocity of $\sim 1\text{--}2$ cm/ns, compared to a c.m. velocity of 2.2 cm/ns. For more forward angles the light particles spray out with higher speed and abundance, but no projectilelike second source is evident. (This pattern contrasts with that for central collisions of 28.2A MeV $^{136}\text{Xe} + ^{209}\text{Bi}$, where apparently isotropic emission seems to occur from two distinct sources [13].) Heavy residual nuclei are also abundantly generated in these central collisions of $^{40}\text{Ar} + ^{\text{nat}}\text{Ag}$; they have average velocities about three quarters of the c.m. velocity [12,14,15]. Mass numbers of these heavy residuals are $A \sim 80$ for the final stable nuclei [14] and $A \sim 115$ for typical highly excited nuclei during the ^4He evaporation cascade [9]. This pattern suggests incomplete fusion giving a very hot nuclear system of initial $A \sim 130$ after a spray of forward peaked, directly emitted particles [8–12,15]. This spray could also be thought of as parts of a projectile fragment shattered in the central collision. Central collisions (i.e., those associated with the largest light-charged particle multiplicities and the production of heavy residual nuclei) have been shown to be strongly selected by the detection of two rare-charged particles (such as d , t , or Li) at $\theta_{\text{lab}} = 32^\circ, 68^\circ$ [11,15]. Therefore, the detection of the particle pairs of interest in this study is autocorrelated with the most central collision group of maximum energy deposition.

Experimental measurements were made of small-angle ejectile pair correlations with the EMRIC [16] 25-detector array at Grenoble using techniques very similar to [10]. Two-particle coincidence events were recorded and used in two ways. Following the usual practice [10], they were binned in relative momentum P_{rel} to form a spectrum $A(P_{\text{rel}})$. A correlation function is defined as the ra-

tio $A(P_{\text{rel}})/B(P_{\text{rel}})$ where $B(P_{\text{rel}})$ is a reference spectrum for the same class of particles but from separate events. We use event mixing for the construction of the reference spectrum $B(P_{\text{rel}})$; this reference spectrum is the area normalized to the total number of events in the real spectrum $A(P_{\text{rel}})$. In addition, we present velocity difference (V_{dif}) spectra between unlike ejectile pairs, ${}^2\text{H}$ -Li and ${}^3\text{H}$ -Li, for opening angle $\gamma < 7^\circ$. The velocity difference spectra probe both the mean lifetimes and the ejectile emission order [7] as discussed below. Trajectory calculations with a detection filter from the reaction simulation code MENEKA [6] are used to interpret the data.

Empirical lifetimes, inferred from correlation functions in relative momentum, describe the mean time interval between ejectile pairs [6]. We follow the common assumption that the time interval distribution involves exponential decay for each ejectile. Therefore, we identify the mean time difference between randomly selected *like* ejectile pairs with the mean lifetime τ for emission of that ejectile. Correlation functions and V_{dif} spectra built from coincidences between *unlike* ejectiles also provide a powerful test for a time delay between the initiation of emission for ${}^2\text{H}$ or ${}^3\text{H}$ particles and that for Li fragments. The existence of a finite time delay before the start of fragmentation might be expected if fragmentation occurs after nuclear expansion, e.g., [1–5]; experimental evidence for such a delay would be very important for our understanding of the dynamics.

As shown in Fig. 1(a) the energy spectra for ${}^2\text{H}$ and ${}^3\text{H}$ measured at $\theta_{\text{lab}} = 32^\circ$ both exhibit a very large high-energy component extending past the beam velocity. The comparison to evaporation model calculations indicates that a substantial fraction of the high-energy ${}^2\text{H}$ (and ${}^3\text{H}$) is nonevaporative. This, along with the time scales discussed below, suggests direct emission. Thus, the high-velocity ${}^2\text{H}$ or ${}^3\text{H}$ particles provide a way to sense the leading ejectile group. Such a directly emitted particle along with a Li fragment provides a natural pair to search for the time delay for nuclear expansion between direct light-charged particle emission and fragmentation [1].

Figure 2 shows correlation functions for high-velocity ${}^2\text{H}$ and ${}^3\text{H}$ pairs and also for all Li pairs; the data are well represented by reaction simulations with decay lifetimes of 60 ± 30 , 30 ± 30 , and 120 ± 60 fm/c, respectively. These simulations employ trajectory calculations which use observed energy spectra for each ejectile, normal nuclear radii, average emitter mass, and velocity from [8–11]. (Reference [6] gives details.) Results are unaffected by uncertainties in the emitter mass or velocity, but the use of an expanded source would lead to shorter lifetimes, as discussed below. The lifetimes for high-velocity ${}^2\text{H}$ and ${}^3\text{H}$ are extremely short, i.e., of the same order as nuclear traversal times; this supports the contention that they are indeed promptly ejected, i.e., from direct reaction processes. Lifetimes have also been determined as a function of velocity for the lower energy ${}^2\text{H}$ and ${}^3\text{H}$ ejectiles [17]; for ${}^2\text{H}$ or ${}^3\text{H}$ energies of

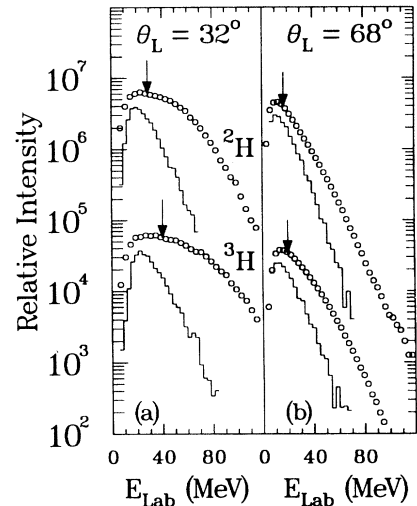


FIG. 1. (a) Energy spectra for ${}^2\text{H}$, ${}^3\text{H}$, observed (a) at 32° and (b) at 68° (open points) compared to statistical model calculations (histograms) as derived from fits to the data at 90° ($a = A/10$, $0 < J < 100\hbar$) as in Refs. [6,7,10]. Arrows indicate the velocity cuts used for Figs. 2–4.

~ 10 MeV, these τ values rise to ≥ 1000 fm/c, presumably due to more extensive thermalization [1]. By contrast, however, hardly any significant change of lifetime (i.e., ≤ 120 fm/c) with velocity was found for the Li [7].

For the unlike ejectile pairs, more definitive information can be gleaned by focusing on the velocity difference spectra, in which sensitivity to emission order (as well as time interval) has been demonstrated [7]. The data points in Fig. 3 show the spectrum of experimental velocity

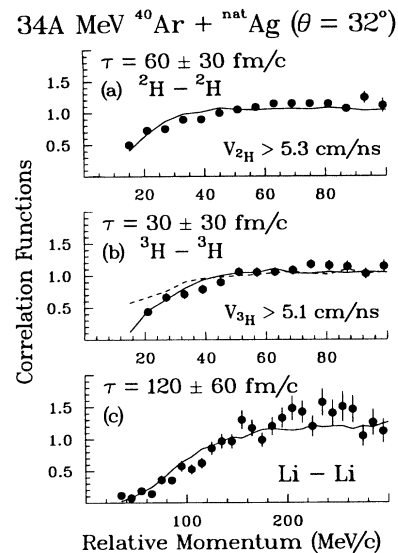


FIG. 2. Correlation functions for coincidences between high-energy ${}^2\text{H}$ and ${}^3\text{H}$ pairs (with velocity cut as indicated in Fig. 1) and all Li pairs. Data are shown as points; calculations [6,7,10] as lines with τ values as indicated. The dashed curve in (b) is for the upper bound of the quoted uncertainty.

differences (actually speed differences) between high-velocity ${}^2\text{H}$ (or ${}^3\text{H}$) and all Li fragments for coincidences with an opening angle $\gamma < 7^\circ$. Note in Fig. 3(a) for ${}^2\text{H}$ -Li [or Fig. 3(e) for ${}^3\text{H}$ -Li] that the observed spectrum has a large bump for $V_{2\text{H}} > V_{\text{Li}}$ and a small one for $V_{\text{Li}} > V_{2\text{H}}$. Trajectory calculations reveal that the magnitudes of these bumps, i.e., the probabilities for detection of coincidence pairs at small relative angles, depend on four aspects: (a) the *ejectile emission order*, (b) the strength of the force between ejectile pairs, (c) the time interval between emissions, and (d) the acceptance of the detectors. In particular, a fast-moving ejectile that overtakes its slower moving (but previously emitted) partner will often scatter or react and be eliminated from detection. By contrast, if the faster moving ejectile is emitted first, then the interaction will be weaker, and the pair has a much better chance for detector acceptance at small relative angle. This feature drives the relative intensities of the spectral bumps on either side of $V_{\text{dif}} = 0$ and thus provides a good probe of the ejectile emission order [7]. In contrast, changes in the mean time delay between particle emission result only in the depletion of a narrow region of the spectrum centered at $V_{\text{dif}} = 0$; time delay does not change the relative spectral intensities on either side of $V_{\text{dif}} = 0$ [7]. Comparison between experimental and simulated distributions of velocity differences can thus be used to investigate the proposed freeze-out delays in the emission of Li fragments [1,2].

The histograms in Figs. 3(a) and 3(c) result from simulation calculations with two different time scale

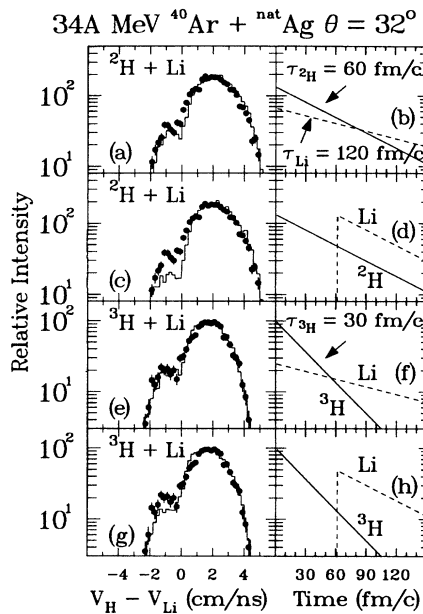


FIG. 3. Velocity difference spectra ($\theta_{\text{lab}} \sim 32^\circ$) for Li in coincidence with high-velocity ${}^2\text{H}$ or ${}^3\text{H}$ ($\gamma < 7^\circ$). Data are shown by points; calculations by lines with associated emission time distributions are shown on the right.

scenarios as indicated in Figs. 3(b) and 3(d). Figure 3(a) gives results for a calculation in which the emission probability curves for ${}^2\text{H}$ and Li begin concurrently [Fig. 3(b)], with mean decay times from Fig. 2. A match of the intensity on both sides of the origin indicates an agreement between the experimental and simulated emission orders. Concurrent emission of ${}^2\text{H}$ and Li with τ values indicated in Fig. 3(b) does indeed reproduce the observed V_{dif} spectrum (and hence the average emission order) rather well [Fig. 3(a)]. This can be contrasted with the second timing scenario in which a delay time of 60 fm/c was imposed on the Li fragments. That scenario, depicted in Fig. 3(d), leads to a clear discrepancy between the simulated and experimental results, as shown in Fig. 3(c). The discrepancy would be even more pronounced if the delay time was longer. Note that adding a small time delay to the emission probability curve for Li [Fig. 3(d)] tends to lengthen the average time interval between the ${}^2\text{H}$ -Li pairs, and this damages the fit by the correlation function. This effect was compensated for by a small decrease in the mean lifetime τ_{Li} from 120 to 60 fm/c. This scenario does indeed account for the correlation function (not shown); however, the calculated velocity difference spectrum shows a significantly poorer fit [Fig. 3(c)] to the relative peak heights, clearly indicating that the ejectile emission order is not well described. Figures 3(e)–3(h) give parallel information for ${}^3\text{H}$ -Li pairs with very similar results.

Hence, an important constraint has been placed on the time delay between direct particle production and the start of fragment emission. We recall that an implicit assumption of many current models (e.g., [1–3]) is that direct particle emission precedes a period of nuclear expansion and equilibration that then leads to the freeze-out of nuclear fragments. In this case, the evidence suggests that very little time delay can be tolerated before fragment emission begins. Fragment formation at $\theta_{\text{lab}} \sim 32^\circ$ would seem to be better described as a part of the preequilibrium emission process similar to that for high-velocity ${}^2\text{H}$ and ${}^3\text{H}$. Energy spectra and angular distributions from [18] for ${}^{14}\text{N}$ projectiles and in this work [7,12] for ${}^{40}\text{Ar}$ are also consistent with this conclusion.

Figure 1(b) shows that the energy spectra for ${}^2\text{H}$, ${}^3\text{H}$ at 68° are much softer than at 32° . Presumably, the collision cascade has been more extensive, and the emission system has moved further toward thermal equilibrium; nevertheless, a significant direct component remains for ${}^3\text{H}$ emission. Following again our procedure for Figs. 2 and 3, we gate on high-velocity ${}^3\text{H}$ to select the most rapidly emitted tritons at $\theta_{\text{lab}} \sim 68^\circ$. Then we examine the V_{dif} spectrum for ${}^3\text{H}$ -Li pairs at $\theta_{\text{lab}} \sim 68^\circ$ as shown in Fig. 4. Once again we find a significantly poorer fit if we add a small time delay before the initiation of Li fragmentation. Thus, even for 68° the Li fragmentation also seems to start concurrently with direct particle emission. (Analysis of the ${}^2\text{H}$ -Li pairs at 68° gives a

consistent result [7], but it is complicated by the mixture of more than one mechanism and decay component for ${}^2\text{H}$ emission.)

All calculations shown in Figs. 2–4 were made with source and ejectile radii characteristic of normal nuclei. As the time interval between particle emission becomes extremely short (i.e., $\lesssim 30$ fm/c), the interaction between particles is also affected by the birth positions of the particles. In other words, for nearly instantaneous emission a larger emission source size can lead to less interaction on average between the emitted particles, in a similar fashion as does time delay between emissions. For longer time intervals (e.g., $\gtrsim 100$ fm/c), calculated correlations become insensitive to this effect of source size and reflect only the delay time (or flight path) between particle emissions. This is because the flight path of the first ejectile becomes dominant over the source radius. However, for nearly instantaneous emission of high velocity deuteron pairs, as shown in Fig. 2(a), a source size of $\gtrsim 8$ times normal nuclear volume can also reproduce the observed relative momentum correlations [7].

There is an inherent ambiguity between scenarios that invoke a short time delay and those that invoke a very large source size. Hence, it is conceivable that ${}^2\text{H}$, ${}^3\text{H}$, and Li ejectiles are all emitted after volume expansion and equilibration. Intuitively, it seems unlikely that emission of such high velocity ${}^2\text{H}$ or ${}^3\text{H}$ occurs only after an eightfold volume expansion and equilibration, but *then* nearly instantaneously (i.e., $\tau \sim 30$ – 60 fm/c). The scenario of direct ${}^2\text{H}$ or ${}^3\text{H}$ emission prior to expansion seems more likely [1]. In either case, simulations that employ an expanded source do not change the emission order effects exhibited by the V_{dif} spectra, and, therefore, our conclusions are not qualitatively affected by the assumed source size.

In summary, we have studied the pattern of time intervals between Li fragments and high velocity (i.e.,

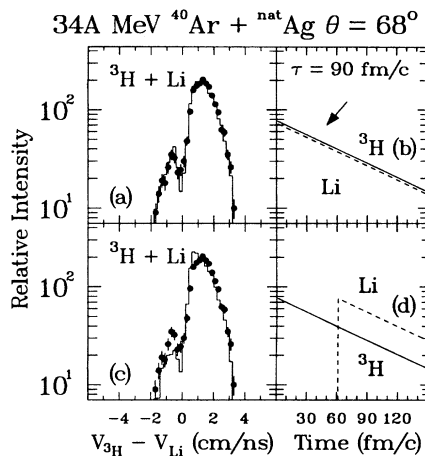


FIG. 4. Same as Fig. 3 but for measurements of ${}^3\text{H}$ -Li pairs at $\theta_{\text{lab}} \sim 68^\circ$. The τ values indicated were obtained from ${}^3\text{H}$ - ${}^3\text{H}$ and Li-Li pairs at 68° with the procedure illustrated in Fig. 2.

direct) ${}^2\text{H}$ and ${}^3\text{H}$ emissions at $\theta_{\text{lab}} \sim 32^\circ$ and $\sim 68^\circ$ using a newly presented experimental observable. In no case can a significant time delay (50 fm/c) be tolerated between high velocity (i.e., direct) emission of ${}^3\text{H}$ or ${}^2\text{H}$ and the initiation of fragmentation to give Li. This conclusion is in apparent conflict with model calculations which predict and/or assume that fragmentation follows a delay time required for nuclear expansion to give a thermalized low density source. Similar study and results for other reactions (particularly at higher excitation energy and where fragments exhibit signatures of equilibration) will be of great value for further elucidation of this crucial aspect of reaction dynamics and the approach to equilibration.

Financial support has been provided in part by the U.S. Department of Energy and by the CNRS of France. M.E.B. and A.M.R. acknowledge partial support from CONACYT, Grant 3173E.

*Present address: Department of Physics, University of Colorado, Boulder, CO 80309-0446.

†Present address: Battelle Memorial Institute, Columbus, OH 43201.

‡Permanent address: Centre d'Etudes de Bruyères-Le-Châtel, Service de Physique et Techniques Nucléaires, Boite Postale No. 12, 91680 Bruyères-Le-Chatel, France.

§Permanent address: Institute de Fisica UNAM, A.P. 20-364, Mexico-01000 DF, Mexico.

- [1] J.P. Bondorf *et al.*, Phys. Rev. Lett. **73**, 628 (1994).
- [2] D.H.E. Gross *et al.*, Ann. Phys. (Leipzig) **1**, 467 (1992).
- [3] D.H.E. Gross *et al.*, Nucl. Phys. **A553**, 175c (1993).
- [4] L.G. Moretto *et al.*, Annu. Rev. Nucl. Part. Sci. **43**, 379 (1992); J. Randrup *et al.*, Prog. Part. Nucl. Phys. **30**, 117 (1993).
- [5] H. Xu *et al.*, Phys. Rev. C **50**, 1659 (1994).
- [6] A. Elmaani *et al.*, Nucl. Instrum. Methods Phys. Res., Sect. A **313**, 401 (1992); A. Elmaani and J.M. Alexander, Phys. Rev. C **47**, 1321 (1993).
- [7] C.J. Gelderloos and J.M. Alexander, Nucl. Instrum. Methods Phys. Res., Sect. A **349**, 618; C.J. Gelderloos, Ph.D. thesis, SUNY at Stony Brook, 1994 (unpublished).
- [8] T. Ethvignot *et al.*, Phys. Rev. C **43**, R2035 (1991).
- [9] T. Ethvignot *et al.*, Nucl. Phys. **A545**, 347c (1992); T. Ethvignot *et al.*, Phys. Rev. C **47**, 2099 (1993).
- [10] A. Elmaani *et al.*, Phys. Rev. C **49**, 284 (1994).
- [11] M.T. Magda *et al.*, Phys. Rev. C **45**, 1209 (1992).
- [12] E. Bauge, Doctoral thesis, Université Joseph Fourier, Grenoble, 1994 (unpublished).
- [13] B. Lott *et al.*, Phys. Rev. Lett. **68**, 3141 (1992).
- [14] B. Borderie *et al.*, Z. Phys. A **338**, 369 (1991).
- [15] M.T. Magda and J.M. Alexander, in *Topics in Atomic and Nuclear Collisions*, edited by B. Remaud (Plenum Publishing Corp., New York, 1994), pp. 97–121.
- [16] F. Merchez *et al.*, Nucl. Instrum. Methods Phys. Res., Sect. A **275**, 133 (1989).
- [17] C.J. Gelderloos *et al.* (to be published).
- [18] M. Fatyga *et al.*, Phys. Rev. Lett. **58**, 2527 (1987).